UNDER PEER REVIEW

AN INVESTIGATION ON SILICONE AND SILICONE RUBBER STENTS IN COMPARISON WITH STAINLESS STEEL STENTS: INTRODUCING A DOUBLE LAYER STENT MODEL

.

ABSTRACT (ARIAL, BOLD, 11 FONT, LEFT ALIGNED, CAPS)

A single layer of different materials; silicone, silicone rubber and steel, is investigated for stent deployment. The response of the proposed stents to simulated radial blood pressure waveform is studied considering the mechanical properties. The stress-strain response and the stored strain energy are computed likewise. Furthermore, a model of a double layer stent made of Silicone-Silicone rubber is suggested. The behavior of the introduced double layer stent model is investigated under the effect of radial pulsating pressure. The model is tested for strain response, stored energy, inertial energy and power losses. This model employs the actual available physical constants. The results indicate that silicon and silicon rubber are not only biocompatible but also eliminate possible thrombosis as well. Moreover, they are electrically compatible as well since they do not contribute to heating complications induced by EMF exposure.

Aims: Study the viscoelastic behavior of an arterial transversally deployed stent, of suggested materials namely silicone and silicone rubber to be compared to the commonly used stainless steel. A proposed double layer stent model stress-strain response is mathematically tested for pulsatile radial pressure.
Study design: Mechanical viscoelastic double layer model
Place and Duration of Study: Faculty of Engineering, Cairo Univ. April to Dec. 2013
Methodology: Computer simulation of the presented mathematical model by MapleV release4 is carried out.
Results: Table 1 shows the results obtained employing the single layer stent model to compare mechanical response of steel, silicone and silicone rubber compared to the inner two layers of the human arterial wall. Silicone and adventitia layers show highest strain responses, 3.98% and 0.54% respectively and consequently largest values of stored energy. Silicone rubber and intima media show strain responses of 0.015% and 0.000603% respectively. These results recommended the proposed design of the double layer stent. Stress-strain complex functions are represented for the each layer besides the stored energy, inertia, and power loss.
Conclusion: Results largely elect the silicone materials to replace steel regarding the strain energy that provides backward pressure. Since stored strain energy contributes to the pulsatile motion of arterial wall then the higher strain lessens susceptibility to possible thrombosis or stagnation. In other words, the pulsating stent wall enhances a vibrating motion that compensates loss of elasticity of a stiff artery. The proposed design for the double layer silicone-silicone rubber stent shows highly fluctuating time response. The fluctuations provide adequate wall strain energy to push back and hence maintain the blood flow rate. This type of stent can be implanted in vessels suffering stiffness to overcome restenosis.

UNDER PEER REVIEW

Keywords: Arterial wall, viscoelasticity, blood pressure, strain response, storage modulus, loss modulus, linear power density.

1. INTRODUCTION

To date, vascular substitutes or stents, have been used for the treatment of arterial blockage. Nevertheless, it has been reported to be a direct factor for restenosis. Estimated rate of in-stent restenosis after deployment of metallic stents in coronary arteries is about 30% [1-3]. Drug-eluting stents have been introduced to lower this effect. Stents, particular metallic ones, usually exhibit mismatch effects due to dramatic differences in mechanical properties. Compliance mismatch between natural artery and implanted metallic stents is reported to be a main possible factor of graft failure, early accumulation of thrombus and later intimal thickening. Compliance mismatch induced by arterial stenting can be reduced by better choice of stent components. Previous investigations have demonstrated that arterial wall compliance and distensibility decreases at stent level. Furthermore, possible thrombosis, usually following arterial stenting, can be reduced by higher stent elasticity [4 - 5].

Previous work showed that compliance and distensibility were significantly lower at the stent level than upstream and downstream by experimental comparison of endovascular stenting. H. Stephan et. al. [6] concluded that there is no stent with ideal physical properties. However, depending on the characteristics of the arterial lesion to be treated, the most appropriate stent can be chosen.

The above tribulations have led scientists to perform in vitro models simulating forces to evaluate quantitative mechanical deformation properties of metallic stents. Elastic and plastic deformation properties of Wallstent, Palmaz stent and Strecker stent were investigated [7]. It was concluded that a purely elastic stent such as the Wallstent is preferable in locations where permanent plastic deformation may occur. While F. Flueckiger et al.[8] held comparisons among five types of expandable metal stents. They reached results that for all types of stresses, the Palmaz stent showed highest resistance. Hence they are appropriate for insertion into highly resistant obstructions whereas Wallstents have expressed unique deformation characteristics and will not function well if implanted into eccentric stenoses of tough consistency. The hoop strength has been tested for different endovascular balloon-expandable metallic stents. C. Tudor et. al. [9] have introduced a study to compare the expansion parameters of four different balloon-expandable stents in a curved stenotic phantom model. Wallstents were positioned in silicon models to study the carotid arterial flow velocities using laser Doppler anemometry [10]. Also results have shown that the flow behavior is affected by the resistance of the stent together with hemodynamically relevant changes.

To overcome some of the expected complications following stent implantation, biocompatible material coating have been introduced to stent materials. In order to lessen the thrombogenicity of the metallic stents D. Klee et. al.[11] devoted their work to coating the metallic stents with an ultra-thin polymer layer. Platelet adhesion is decreased as a result together with improvement of hemocompatibility especially after treatment with sulphur dioxide plasma. Also recent *in vivo* and *in vitro* research work has focused on materials that will reduce encrustation and bacterial biofilm formation for uteral stents [12]. Besides, bioresorbable, expandable poly L-lactic acid stent has been designed [13]. Furthermore, a polymeric flexible aortic and mitral valve prostheses were tested in vitro for durability of PCU (Polycarbonate urethane) valves [14].

Nevertheless, the importance of the study of mechanical properties of the natural arterial layers have haunted scientists for years. They have been concerned with mechanical and mathematical simulation to produce stress-strain relation for different human soft tissues. Yu Q. et al. [15] evaluated the force-deformation relations for different layers of blood vessels

UNDER PEER REVIEW

by studying the non axis symmetric deformation of the vessel wall. Young's modulus is given for the intima media and the adventitial layers of the thoracic artery. The circumferential stretch and axial stretch of abdominal arteries are given for different pressure values by Schulz-Bauer et al. [16] for both normal and hypertensive patients. They proposed a method to determine nonlinear constitutive models for human arteries from clinical data using a strain energy function. Mechanical properties are obtained by reliable experimental setups especially for different arterial layers, collagen and body tissues [17]. The degree of nonlinearity and blood vessel elasticity was studied by J. Zhou and Y. C. Fung [18] introducing a pseudo strain energy function and fitting experimental data to produce its parameters. Furthermore the relationship between wall shear stress and intimal thickening for the abdominal aorta was determined by Micheal Bonert et al.[19], who measured experimentally the wall shear stress using the laser photochromic dye tracer technique. Imaging the mechanical properties of thrombosis, plaques and arterial wall can aid in characterizing and understanding of the pathogenesis of the cardiovascular disease. Intravascular ultrasound is a widely used method of elasticity imaging of the coronary arteries. Strain and elasticity are formulated both mathematically and experimentally to determine mechanical properties of arterial tissues [20-25].

Previous work by the author, [26-27], introduced a viscoelastic mathematical model that represents a section of a blood vessel. Some mechanical properties for two inner arterial layers, namely intima and adventitia, were hence deduced. These properties were adopted therein to reproduce elasticity moduli, both loss and storage for each layer. Stress and strain time responses were represented for these layers.

The present work introduces a stent section made of biocompatible materials that enjoy suitable compliance and distensibility. A comparison of silicone, silicone rubber and steel cylindrical sections with dimensions similar to those of arterial stents is held. Periodic biphasic pressure pulses simulate the radial component of the arterial pressure on the inner stent wall. Though *in vivo* reported pulses show faster rise and fall decay with asymmetry [25], they are represented here with symmetric exponential rise and fall decay functions [26]. Investigation of the three materials concerns strain time response, strain energy, power loss and inertial energy. Comparison shows better response for more elastic materials.

The present work also introduces a double layer of silicone - silicone rubber tubular section as a stent model. The introduced model is expected to reduce restenosis and enhance the upstream in its neighborhood. It is expected not only to reduce blockage, but to compensate for loss of elasticity as well. Loss of elasticity caused mainly by aging leads to hypertension and heart muscle exhaust. Besides being biocompatible, the silicone and silicone rubber are mechanically compatible as well. In other words, systolic-diastolic diameter changes are better sustained when elastic materials are employed. Hence, they represent a better choice for stent manufacture in order to overcome the compliance mismatch. Their relatively low elasticity moduli grant the advantage of being closer to the native arterial response. The calculated strain energy stored per cycle proves to greatly improve in this case. The proposed mathematical model is employed to record the stent response considering the mechanical properties, in response to blood pressure simulated input. A Fourier series represents the radial blood pressure component on the inner wall. The radial response of the stent wall is represented both mathematically and graphically

2. METHODOLOGY

2.1 SINGLE LAYER STENT

The cylindrical section under investigation, fig.1, is 1cm in length. The radial component of the blood pressure pulsates on the inner wall isotropically.

UNDER PEER REVIEW

The stent inner radius, r_1, is 2mm and outer radius, r_2, is 2.1mm. A simplified model, introduced earlier [12], simulates the viscoelastic behaviour of a single layer blood vessel in response to radial blood pulses acting on its inner wall. The single layer stent is treated as a parallel dashpot-spring system to simulate the viscoelastic behavior [25]. The mechanical representation, is analogous to an electrical circuit (appendix1).

The model is tested for three different materials namely, silicone, silicone rubber and stainless steel. The circuit transfer function depends greatly on the elasticity Hooke's constant, *K*, viscosity coefficient, *B*, and mass density ρ_I, summed up in Table 1. Though real pressure pulses are of asymmetric nature [25], they are assumed to be biphasic symmetric pulses. The model assumes almost the same time interval as natural pulses where periodic time, *2T,* is *1s*. The exponential rise and decay pulse components are assumed to have equal decay constants. A Fourier series is generated to represent the radial pressure, $P_r(t)$, shown in fig.(2),[27].

$$P_r(t)=\frac{2}{\pi}P_0\sum_{n=1}^{\infty}\frac{(e^{-\pi}(\cos n\pi-1)-(\cos n\pi+1))\cos\frac{n\pi t}{T}}{+\frac{1}{n}(e^{-\pi}(\cos n\pi-2)-(\cos n\pi+1))\sin\frac{n\pi t}{T}-\frac{1}{n}e^{-\pi}\cos n\pi} \quad (1)$$

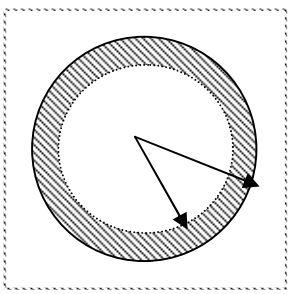

Fig.1. The single layer stent

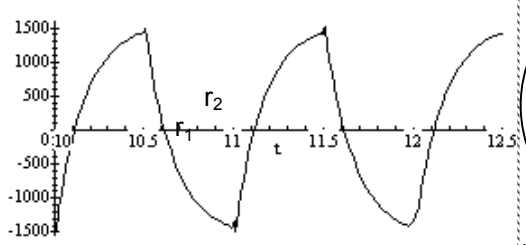

Fig. 2. Exponential Rise and fall of the radial pressure in Pa Vs. time(s)

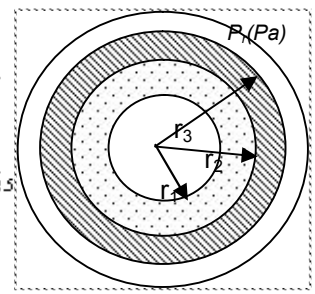

Fig.3. The double layer stent

2.2 Double Layer Stent

The double layer viscoelastic model introduced earlier [27] is extended for further study. The silicone -silicone rubber double layer stent is represented in fig.(3) as a double layer uniaxial cylindrical section. The inner radius of the silicone layer, r_1, is assumed to be 2mm. The outer radius of the silicone rubber layer, r_2, is 2.2mm. The response of both layers is studied simultaneously. The double layer silicone-silicone rubber stent is treated as a double section R-L-C circuit (appendix 1) equivalent to the mechanical viscoelastic model. The transfer function, Y(s), depends on the mechanical properties of both layers. These are summed up in Table 2.

UNDER PEER REVIEW

3. Mathematical Analysis

The mathematical representation of pressure pulses, $P_r(t)$, eq.(1) is employed in the viscoelastic model as the input pressure on r_1, assuming maximum value P_o, to be 10% of the average blood arterial pressure in adults. Analogy between the mechanical system and the equivalent electrical circuit is shown in appendix 1. It is noteworthy that the stress on a specific wall is the difference in pressures across its boundaries. Thus the stress on the inner layer, $T_1(t) = P_1(t)-P_2(t)$, and $T_2(t)=P_2(t)-P_3(t)$ are the stresses on the outer layer where $P_1(t)=,P_r(t)$, P_2 on the interface between the two layers and P_3 is the stress on the boundary. Consequently, the strain functions are calculated as: $\varepsilon_1(t)=(r_2(t)-r_1(t))/r_1(t)$, $\varepsilon_2(t)=r_3(t)-r_2(t)/r_2(t)$ for respective layers. The second order differential equations that govern the strain functions, ε_1(t) and ε_2(t) of both layers and the inertial forces acting on them are as follows:

$$\frac{d^2 r_1(t)}{dt^2} = F_1(t) - B_1 \frac{dr_1(t)}{dt} - K_1 r_1(t) \qquad \frac{d^2 r_2(t)}{dt^2} = F_2(t) - B_2 \frac{dr_2(t)}{dt} - K_2 r_2(t) \qquad (2)$$

where $B_1=B_1`/\rho_{t1}$ , $K_1=K_1`/\rho_{t1}$, $B_2=B_2`/\rho_{t2}$ , $K_2=K_2`/\rho_{t2}$, are viscosity coefficients and elasticity constants normalized to the linear mass densities, ρ_{t1}, ρ_{t2} for inner and outer layers respectively. $F_1(t)$ and $F_2(t)$ are defined as the normalized radial components of the respective forces. These forces are generated due to radial blood pressure pulses, $P_1(t)$, pulsating on the inner layer producing successive pulses $P_2(t)$, on the interface between the layers.Hence the mathematical formula representing the radial strain function governing its dependence on the wall viscoelastic properties is:

$\varepsilon_1(t)=\Delta r(t)/r_1$ where $\Delta r(t)=r_2(t)-r_1(t)$
and $r_1(t)=(r_1'(t)+r_1''(t)+r_1'''(t))$

$$r_1'(t) = \sum_{n=1}^{\infty} \frac{\rho_{l1}(e^{-\pi}(\cos n\pi - 2)-(\cos n\pi+1))}{} \times\{\frac{\cos(n\omega t-\delta_1)}{\sqrt{B_1^2\omega^2+(K_1-\omega^2)^2}}+\frac{e^{-1/2 B_1 t}}{B_1^2\omega^2+(K_1-\omega^2)^2} \times(\frac{K_1^2+\omega^2}{2\delta_{01}}\sin\delta_{01}t+K_1(K_1+\omega)^2\cos\delta_{01}t)\}$$

$$r_1''(t) = \sum_{n=1}^{\infty} \frac{\rho_{l1}}{n}(e^{-\pi}(\cos n\pi-2)-(\cos n\pi+1)) \times\{\frac{\sin(n\omega t-\delta_1)}{\sqrt{B_1^2\omega^2+(K_1-\omega^2)^2}}+\frac{\omega e^{-1/2 B_1 t}}{B_1^2\omega^2+(K_1-\omega^2)^2} \times(\frac{2\omega^2+B_1^2-2K_1}{2\delta_{01}}\sin\delta_{01}t+B_1\cos\delta_{01}t)\}$$

$$r_1'''(t) = \sum_{n=1}^{\infty}\frac{\rho_{l1}}{n}e^{-\pi}\cos n\pi\{\frac{4}{B_1^2+\delta_0^2}+\frac{\lambda_1\omega e^{-1/2 B_1 t}}{\sqrt{B_1^2-4K_1}}(\frac{e^{i\delta_{01}/2}}{\delta_{11}}-\frac{e^{-i\delta_{01}/2}}{\delta_{12}})\} \qquad ....(3)$$

UNDER PEER REVIEW

where $\omega = \pi/T$, $\lambda_1 = 2\pi\, r_1\, P_0 / \rho_{l1}$, $\delta_1 = \tan^{-1}(B_1\, \omega /(K_1 - \omega^2))$, $\delta_{01} = ½(4K_1 - B_1^2)^{1/2}$ and $\delta_{11,12} = -½(B_1 \pm i\delta_{01})$. The variables δ_1 and δ_{01} can be defined as the phase lag angle as the harmonics angle of the inner layer respectively. Furthermore, the strain energy density, $e_1(t)$, the inertial energy per unit length, $i_1(t)$, and the power loss density, $W_1(t)$, can be calculated for each layer as follows: $e_1(t) = ½P_1(t)\, \varepsilon_1(t)$ $\quad i_1(t) = ½\, \rho_{l1}\, (dr_1(t)/dt)^2$ $\quad W_1(t) = ½B_1\, (dr_1(t)/dt)^2$ ...(4)

One can deduce similar formulae for $\varepsilon_2(t)$, $e_2(t)$, $i_2(t)$, $W_2(t)$.

4. RESULTS AND DISCUSSION

4.1 SINGLE LAYER STENT

The input pulsating blood pressure simulates the natural arterial pulse as an exponential rise exponential decay waveform with frequency nearly equals to average pressure pulse duration. Periodic time, *2T*, equals to *1s*. The *RMS* value of the pulsating radial pressure is *1.322kPa* and peak value is, P_0=*1.6kPa*. The mechanical properties, namely *B*, *K* and ρ_l, together with calculated *RMS* values of the strain function, ε_{rms}, and the calculated strain energy density, *e(t)* are tabulated in Table1. For the sake of a better comparison, the natural inner arterial layers, intima media and adventitia, are investigated similarly. Their mechanical properties employed here are those deduced earlier [27]. This time vibration or the strain response, *ε(t)*, is represented graphically against time(s) for each of the selected materials in fig.4. The strain energy density, *e(t),* variation with time (s) is represented in fig.5. While the time variation of the inertial energy density, *I(t)*, (J/cm^3) is represented in fig.6 . Fig.7 shows that of power loss density, *W(t)*, (watt/cm^3).

Table 1
Data sets for different materials

Material	B gs^{-1}	K N/m	ρ_l g/m	ε_{rms} 10^{-4}	$e(t)$ J/m^3
Silicone	20.573	16.328×10^4	29.39	397.97	26.42
Silicone rubber	29.642	12.874×10^5	29.642	1.496	0.09888
Steel	29.3904×10^3	12.56×10^{10}	195.936	0.0005214	0.3446×10^{-4}
Intima media	10.00	22.23×10^4	25	0.06029	0.3985×10^{-2}
Adventitia	5.004	0.6×10^3	12	54.5	3.6025

UNDER PEER REVIEW

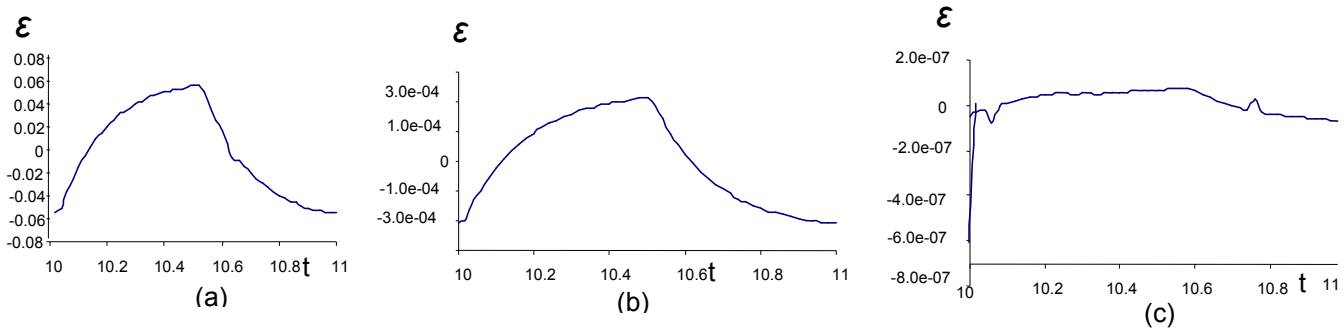

Fig.4. Strain versus time (s) for a) Silicone b)Silicone rubber c) Steel

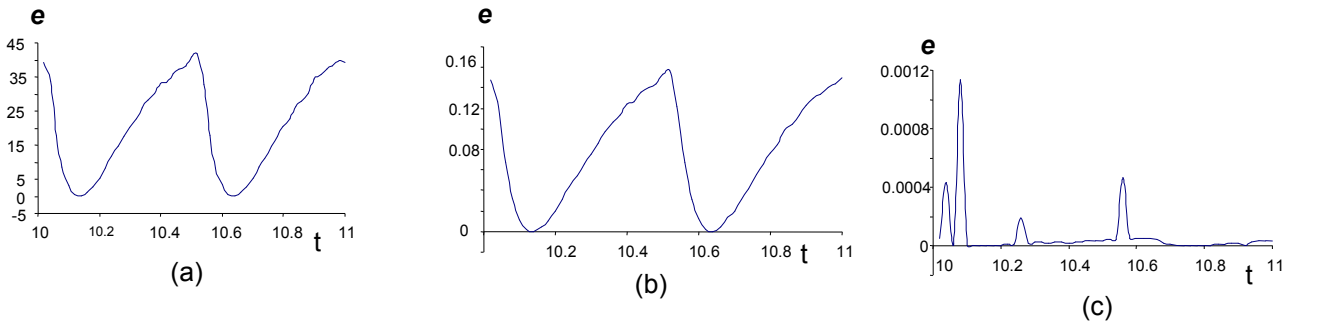

Fig.5. Strain energy density (μJ/cm^3) versus time (s) for a) Silicone b) Silicone rubber c) Steel

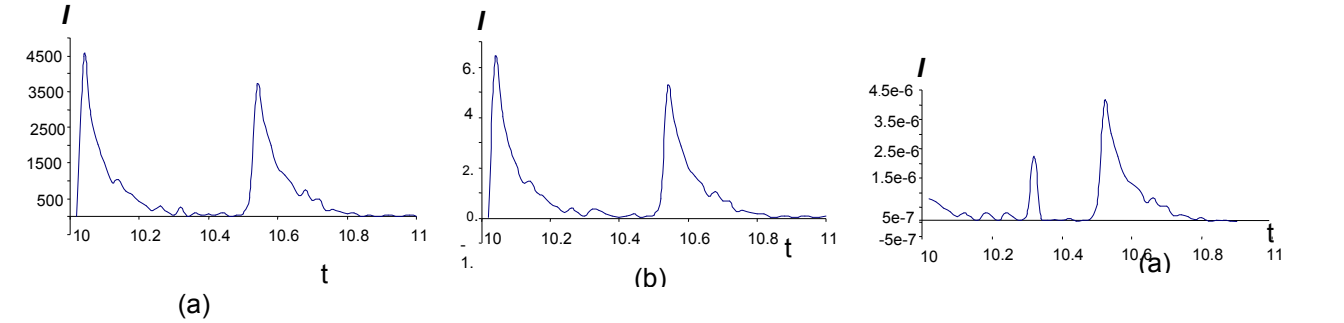

Fig.6. Inertial energy density (μJ/cm^3) versus time (s) for a) Silicone b) Silicone rubber c) Steel

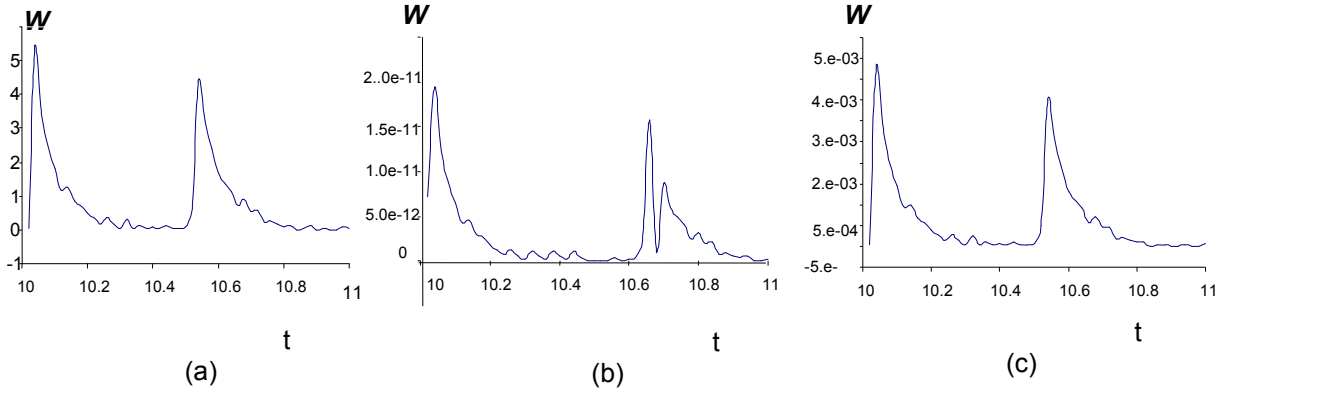

UNDER PEER REVIEW

Fig.7. Power loss density (watt/cm^3) versus time (s) for a) Silicone b) Silicone rubber c) Steel

4.2 DOUBLE LAYER STENT

The double layer stent shown in fig.(3) is modeled mathematically under the pulsating blood pressure simulation shown in fig.(2). The complex strain function of the inner silicone layer in response to the inner radial stress, $P_1(t)$, and that of the outer silicone rubber layer in response the stress relayed to it, $P_2(t)$, are hence computed. The mechanical properties employed during computations are tabulated in Table2, together with the *RMS* value of the strain for each layer. Their viscoelastic responses to the exponential rise exponential decay radial stress applied are shown in the figures below.

Table 2
Mechanical Properties for the double layer stent

Layer	B gs^{-1}	K 10^4 N/m	ρ_l g/m	ε_{rms} 10^{-3}
Silicone	20.573	16.328	29.39	39.79
Silicone rubber	29.642	128.74	29.642	0.1496

The real and the imaginary components of the radial stress acting on each layer and hence its strain response are shown in figs.(8), (9), (10), (11).

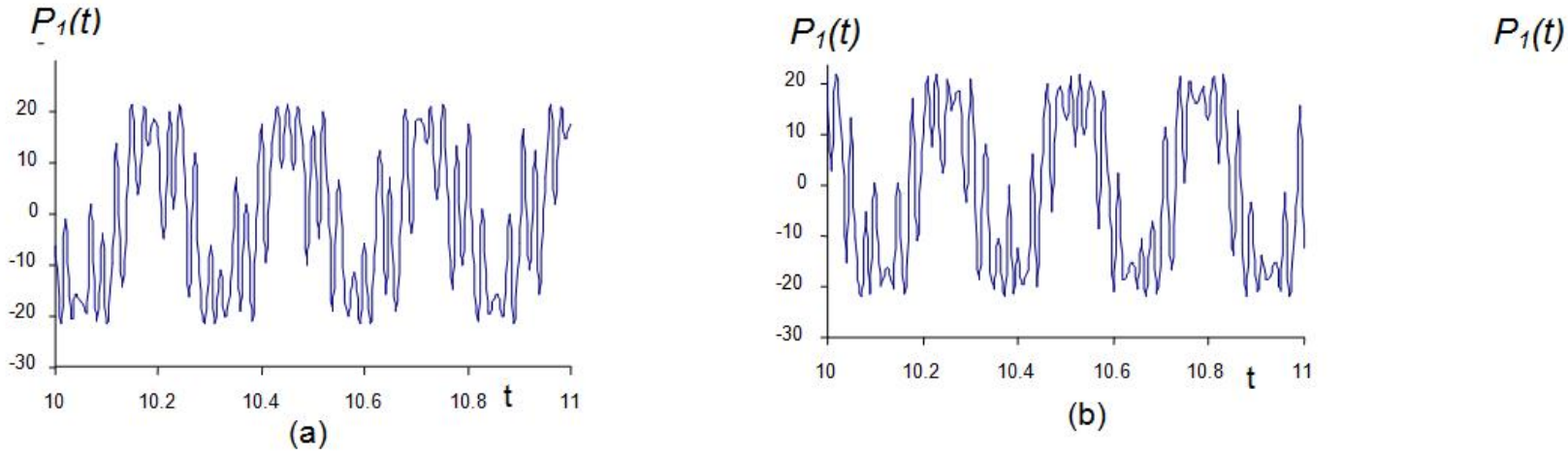

Fig.8. Stress (Pa) versus time (s) on the inner silicone layer a) Real b) Imaginary

Fig.9. Strain versus time (s) on the inner silicone layer a) Real b) Imaginary

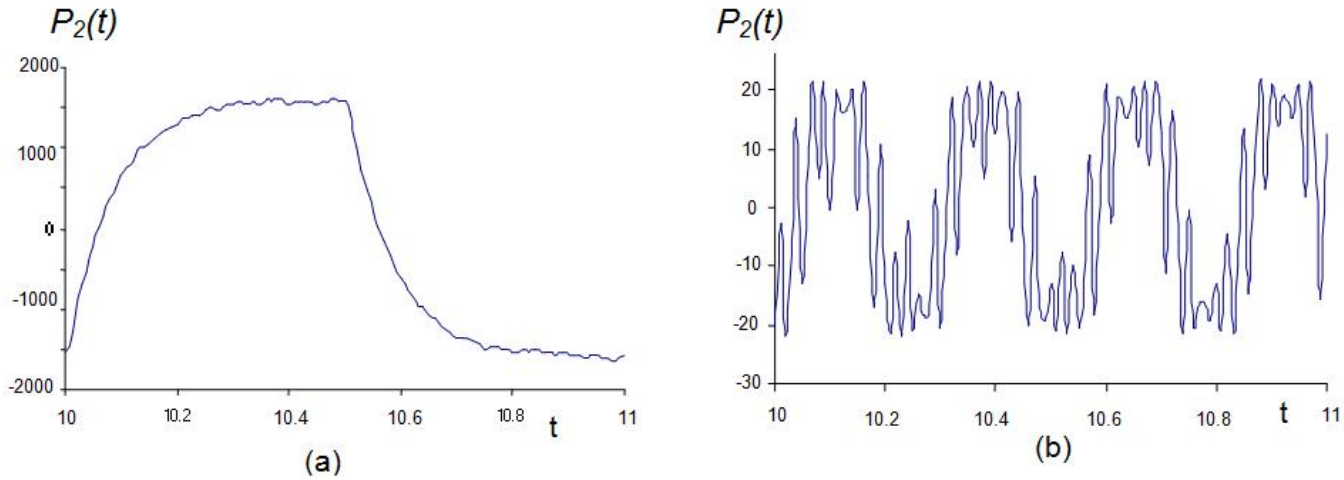

Fig.10. Stress (Pa) versus time (s) on the outer silicone rubber layer a) Real b) Imaginary

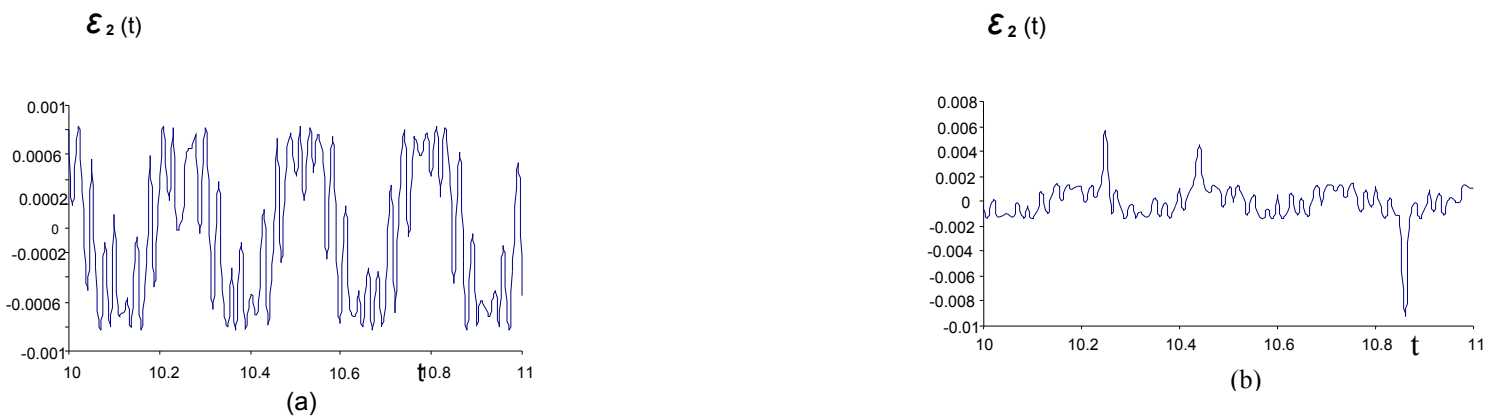

Fig.11. Strain versus time (s) on the outer silicone rubber layer a) Real b) Imaginary

The real and the imaginary components of the strain energy density and inertial energy density on inner and outer stent layers are shown in figs.(12), (13), (14), (15) respectively.

Fig.12. Strain energy density (μJ /cm3) versus time (s) stored in the inner silicone layer a) Real b) Imaginary

Fig.13. Strain energy density (μJ /cm3) versus time (s) stored in the outer silicone rubber layer a) Real b) Imaginary

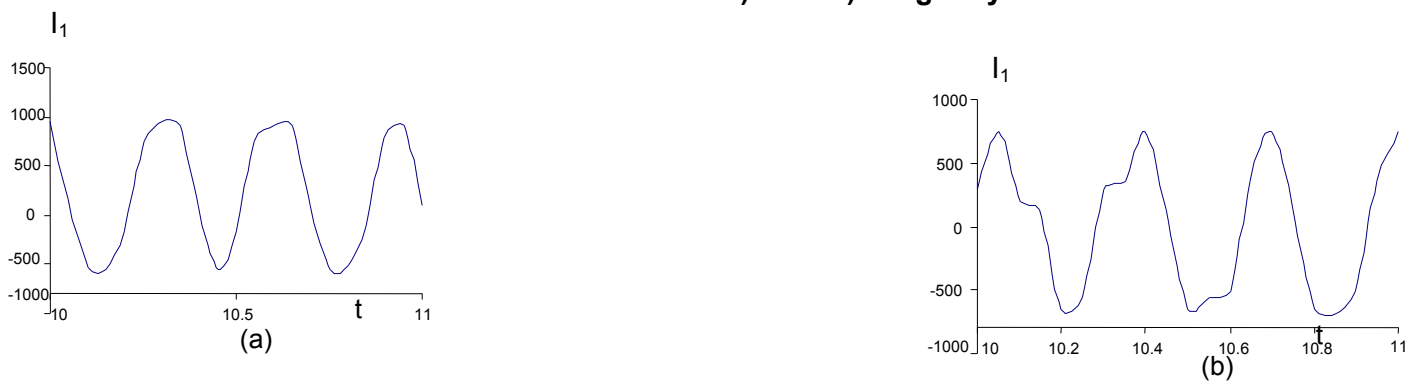

Fig.14. Inertial energy function (μJ/cm3) versus time (s) stored in the inner silicone layer a) Real b) Imaginary

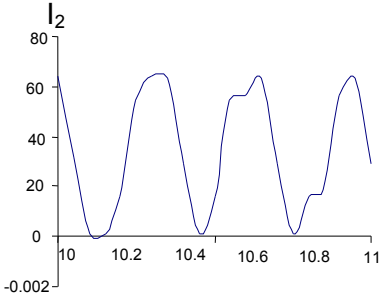

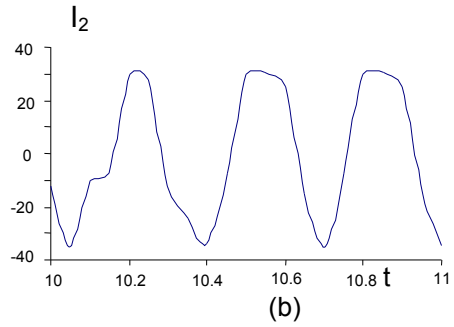

Fig.15. Inertial energy function (μJ/cm3) versus time (s) stored in the outer silicone rubber layer a) Real b) Imaginary

UNDER PEER REVIEW

5. CONCLUSION

Results largely elect the silicone materials to replace steel regarding the strain energy that provides backward pressure. Since stored strain energy contributes to the pulsatile motion of arterial wall then the higher strain lessens susceptibility to possible thrombosis or stagnation. In other words, the pulsating stent wall enhances a vibrating motion that compensates loss of elasticity of a stiff artery. The proposed design for the double layer silicone-silicone rubber stent shows highly fluctuating time response. The fluctuations provide adequate wall strain energy to push back and hence maintain the blood flow rate. This type of stent can be implanted in vessels suffering stiffness to overcome restenosis.

An extra advantage of the use of silicon and silicon rubber as stents is that these materials are chemically inert which is essential for long term implementation in the human body. Moreover, they are electrically inactive either for ionic interaction with the flowing blood or possible interaction with electromagnetic penetrating radiation. C. Zhaojin and W. Qiang [28] among others have indicated that EMF exposure can lead to some harmful effects on the cardiovascular function, it may influence the electrophysiological activities, blood pressure, ..etc. The magnetic and electric field components accompanying any microwave radiation emitted by mobile phones or other similar devices greatly affect the stainless steel stent. These nearby generated fields being incident on a conducting metallic stent section cause an induced EMF. This causes disturbance in the plasma flow leading to non uniformity of flow or trapping of ionic components such as H^+, OH^-, Ca^{++}, Na^+ ,Cl^-,…etc. along the stent length.

As for the heating effect of EMF radiation in frequency ranges of (3kHz-30GHz), should also be considered. Stainless steel, having high thermal conductivity coefficient, transfers higher amount of heat energy. Power transmitted by a single mobile phone, for example, is in the order of magnitude of (100-400mW/cm^2) per device[28]. For a 2mm radius and 5mm length stent, the power absorbed is in the order of (62.8 mW-251.2 mW) [29]. Considering the extensive use of microwave in different technological applications, this power may exceed the permissible limits and lead to local elevation of temperature around the metallic stent.

Conclusively, it is recommended to replace the conventional material of stents by the ones proposed in this paper. We believe that they will maintain to great extent the mechanical functionality of the arterial wall storing elasticity that prevent blood stagnation around the stent. They also offer better chemical and electrical compatibility of the system besides biocompatibility. We are currently devoting efforts on evaluating the EMF interaction with the proposed materials in more details.

COMPETING INTERESTS

“Authors have declared that no competing interests exist.”.

REFERENCES

1. D.L. Fischman, M.B. Leon, et al., "A randomized comparison of coronary stent placement and balloon angioplasty in the treatment of coronary artery disease", New Engl. J. Med., Vol.331, pp.496-501, 1994.

2. P.W. Serruys. P. de Jaegere, et al., "A comparison of balloon-expandable-stent implantation with balloon angioplasty stent (Pa)tients with coronary artery disease", New Engl. J. Med., Vol.331, pp.489-495, 1994.

UNDER PEER REVIEW

3. T. Rau, J. Schofer, et al., "Stenting of non acute total coronary occlusions: predictors of late angiographic outcome", J. Am. Coll. Cordiol , Vol.31, pp.275-280, 1998.

4. F. Nicoud, H.V. Kovacsik, et al., "Arterial stenting: From hemodynamics and wall mechanics to restenosis-Experimental in vivo and theoretical approaches", CNRS UMR5149 I3M, Universite Montpellier II, France, Internet communication.

5. H. Vernhet, R. Demaria, et al., "Changes in Wall Mechanics After Endovascular Stenting in the Rabbit Aorta:Comparison of Three Stent Designs ", American Roentgen Ray Society, *AJR,* Vol.176, pp. 803-807 *,* 2001

6. H. Stephan., M. D. Duda, , et. al., **"**Physical Properties of Endovascular Stents: An Experimental Comparison" , Department of Radiology, Eberhard-Karls-Universität Tübingen, Germany; and Nitinol Devices & Components (D.S.), Fremont, California, Internet communication.

7. S.V. Lossef, RJ Lutz, et. al. , " Comparison of mechanical deformation properties of metallic stents with use of stress-strain analysis" Journal of Vascular and Interventional Radiology, Vol 5, Issue 2, pp. 341-349, 1994.

8. F. Flueckiger, H. Sternthal, et. al., **"** Strength, elasticity, and plasticity of expandable metal stents: in vitro studies with three types of stress", Journal of Vascular and Interventional Radiology, Vol 5, Issue 5, pp. 745-750, 1994.

9. C.Tudor MD Poerner**,** et. al., **"**Determinants of Stent Expansion in Curved Stenotic Lesions: An In Vitro Experimental Study"**,** Journal of Vascular and Interventional Radiology, Vol.15, pp.727-735, 2004.

10. M.D. Oliver Greil, P. Gottlieb, et. al., **"**Changes in carotid artery velocities after stent implantation: A fluid dynamics study with laser Doppler Anemometry"**,** J. of Vascular and interventional Radiology**,** Vol. 5, No. 2, pp.341-349, 1994.

11. J.Lahann D.Klee, H. Thelen, et. al., **"**Improvement of hemocompatibility of metallic stents by polymer coating"**,** J. of Materials Science: Materials in Medicine**,** Vol. 10, No. 7, pp.443-448, Jul 1999.

12. J.D. Denstedt, G. Reid, et. al., **"**Advances in uteral stent technology "**,** World Journal of Urology**,** Vol. 18, No. 4, pp.237-242, Sept. 2000.

13. S.Shih-Horng, Y.N. C. Robert, et. al., **"**New flexible polymeric heart valve prosthesis for the mitral and aortic positions"**,** The Heart Surgery Forum**,** Vol. 7, No. 5, pp.525-532, Oct. 2004. [14] A.Korpela, P. Aarnio, et. al., **"**Bioabsorbable Self-reinforced Poly-L-Lactide, Metallic, and Silicone Stents in the Management of Experimental Tracheal Stenosis"**,** American colledge of chest physicians, Vol. 115, pp.490-495, 1999.

15. Yu Q,Zhou J, and Fung Y C, "Neutral axis location in bending and Young's modulus of different layers of arterial wall", Am J Physiol, H52-60, p 265, Jul 1993.

16. Schulze-Bauer and Holzapfel, J. Biomechanics, 2003, Internet communications.

17. Y. C. Fung, "Mechanical properties of living tissues", Springer, New York, second edition, 1993.

18. J. Zhou. and Y. C. Fung, "The degree of nonlinearity and anisotropy of blood vessel elasticity", Proc. Natl. Acad. Sci. USA Vol. 94, pp. 14255-14260, Dec. 1997.

19. Charles Choi, Biomedical Engineering Dept., Biomedical Ultrasonic lab., Univ. of Michigan, internet communication.

20. Mingxi Wan, Yangamei Li, Junbo Li Yaoyao Cui, and Xiaodong Zhou, "Strain imaging and Elasticity Reconstruction of Arteries Based on Intravascular Ultrasound Video Images" IEEE Transactions on Biomedical Engineering, Vol. 48, No. 1, 2001.

UNDER PEER REVIEW

21. S. Cirovic, C. Walsh, W. D. Fraser, "A model of pulse transmission in the intracranial arteries", Internet communications.

22. T.Shishido, M. Sugimachi, O. Kawaguchi, H.Miyano, T. Kawada, W. Matsuura, Y. Ikeda, T. Sato, J. Alexander Jr., and Kenji Sunagawa, "A new method to measure regional myocardial time-varying elastance using minute vibration", Am J Physiol Heart Circ Physiol, Vol. 274, issue 4, H1404-H1415, April 1998.

23. Mette S. Olufsen, "Structured tree outflow condition for blood flow in larger systemic arteries. " Am J Physiol Heart Circ Physiol, Vol. 276, issue 1, H257-H268, January 1999.

24. Ed VanBavel, Pier Siersma, and Jos A.E.Spaan, "Elasticity of Passive Blood Vessels: A New Concept", Am J Physiol Heart Circ Physiol, Vol.10, July 2003.

25. Harold J. Metcalf, " Topics in Classical Biophysics", Prentice-Hall, inc., New Jersey, May 1979

26. M. A. El-Naggar, and M. A. El-Messiery, "The viscoelastic response of blood vessels under the effect of pulsating pressure", Proceedings of the biological effects of the EMFs, 3rd international workshop, Kos, Greece, Vol.11, pp.50-55, Oct. 2004.

27. M. A. El-Naggar, "A double layer arterial wall model under pulsating blood pressure", Proceedings of the biological effects of the EMFs, 4th international workshop, Crete, Greece, Vol.1, pp. 1412-1418, Oct. 2006.

28. C. Zhaojin and W. Qiang, “Epidemiological studies of EMF health effects in Chine: A review of recent studies”, 3rd International EMF seminar in China , Electromagnetic Fields and Biological Effects, Guilin China, Oct. 2003.

29. K. Tahata, et. al., Engineering in Medicine and biology Society, Proceedings of the 25th annual international conference of the IEEE, Vol.4, pp.3360-3363, Sept.2003

APPENDIX

UNDER PEER REVIEW

The second order differential equations that govern the electrical charge, q , with circuit components, R,L,C, and input voltage V_0 is:

$$\frac{d^2 q(t)}{dt^2} = V_0(t)/L - \frac{R}{L}\frac{dq(t)}{dt} - \frac{1}{LC}q(t) \tag{9}$$

$q_1(t)$, $q_2(t)$ and $q_3(t)$ are the equivalent charges in analogous circuit. By analogy between the two systems, mechanical and electrical, note that:

$V_0(t) \leftrightarrow 2\pi P_1(t)$,

$R/L \leftrightarrow B$

$1/LC \leftrightarrow K$

$L \leftrightarrow \rho_\ell$

Since $P_1(t)$, $P_2(t)$ and $P_3(t)$ are analogous to V_1, V_2 and V_3, thus we can deduce the involved quantities in the s-domain as follows:

$$I_1(s) = Y_{eq}(s)V_1(s) \tag{6}$$

where Y_{eq} represents the total admittance of the two circuit section.

$$V_2(s) = V_1(s) - I_1(s)(R_1 + \frac{1}{sc_1})$$

$$V_3(s) = V_2(s) - I_3(s)(R_2 + \frac{1}{sc_2}) \tag{7}$$

Furthermore, the equivalent resistance, Req, can be introduced as the impedance component responsible for the dissipated energy per pulse per meter, e_{diss}. Whereas the equivalent reactance, Xeq, is the impedance component responsible for the stored energy per pulse per meter, e_{st} . These can be deduced as follows:

$$e_{diss}(\mathrm{t}) = \frac{1}{T}\int_0^T i_1^2(t)R_{eq}\,dt, \quad e_{st}(\mathrm{t}) = \frac{1}{T}\int_0^T i_1^2(t)X_{eq}\,dt \tag{8}$$